Biophysical Chemistry 152 (2010) 46–54

Contents lists available at ScienceDirect

Biophysical Chemistry

journal homepage: http://www.elsevier.com/locate/biophyschem

Budding of giant unilamellar vesicles induced by an amphitropic protein β_2-glycoprotein I

Jasna Kovačič [a,*], Bojan Božič [a], Saša Svetina [a,b]

[a] Institute of Biophysics, Faculty of Medicine, University of Ljubljana, Ljubljana, Slovenia
[b] Jožef Stefan Institute, Ljubljana, Slovenia

ARTICLE INFO

Article history:
Received 17 June 2010
Received in revised form 26 July 2010
Accepted 28 July 2010
Available online 3 August 2010

Keywords:
β2-glycoprotein I
Amphitropic proteins
Phospholipid vesicles
Vesicle budding

ABSTRACT

β_2-glycoprotein I (β_2GPI) is a plasma protein capable of binding reversibly to membranes, and is classified among the amphitropic proteins. Part of the protein intercalates into the outer membrane leaflet, altering the difference between the preferred areas of the membrane leaflets, which results in membrane shape transformations. Budding, as a specific example of such shape transformations, was studied using giant unilamellar vesicles. Our aim was to identify the vesicle parameters that influence the degree of membrane budding by studying this process qualitatively and quantitatively. A simple theoretical model has been developed and assessed against the experimental observations. The results show that β_2GPI binds in a concentration dependent manner, causing transitions between vesicle shapes with increasing numbers of buds. Higher numbers of buds are characteristic of larger and/or more flaccid vesicles. When the vesicle membrane is strained, a higher β_2GPI concentration is needed to produce the same effects as on the unstrained vesicle. Vesicles were found to be highly individual in their behaviour, so each was treated individually. Specific vesicle behaviour was found to be the consequence of the neck between the main vesicle body and the buds, which could be either open, closed for the exchange of solution, or closed for the exchange of both solution and membrane.

1. Introduction

The class of proteins defined as amphitropic [1] can translocate reversibly from the cytosol/plasma into the membrane of cells. Three membrane binding motifs have been proposed and described in detail [2]: (i) a lipid clamp that regulates the association of a protein with a specific lipid headgroup, (ii) a covalently bound lipid anchor that embeds in the membrane and (iii) an amphipathic helix that is embedded in the membrane parallel to the membrane surface, in such a way that the hydrophobic face of the helix orients towards lipids and the polar face to the aqueous phase. β_2-glycoprotein I (β_2GPI) is an amphitropic protein of type (iii) but a structurally distinct binding motif with a patch of positive charges and a hydrophobic loop inside this patch.

β_2GPI is a 50 kDa plasma protein. Its crystal structure reveals five domains connected in an elongated fish-hook shape (Fig. 1a). While the first four domains are regular short consensus repeats, the fifth domain differs structurally and functionally [3]. It contains a 20 nm^2 large patch containing 14 positively charged amino acid residues and a hydrophobic loop that consists of seven amino acid residues. The loop is approximately 1.5 nm long, 1.2 nm wide and 0.9 nm deep (Fig. 1a), and the area of the cross-section of the loop of about 1 nm^2. These characteristics indicate that the fifth domain is implicated in the membrane binding which is mediated by strong electrostatic interactions between its positive charges and the negative charges of the lipid polar headgroups [4]. Binding of β_2GPI does not take place in the absence of the latter. The affinity increases with increasing molar fraction of negatively charged lipids in the membrane and decreases with increasing ionic strength of the medium [5–9]. The association is further strengthened by hydrophobic interactions in which the hydrophobic loop of the fifth domain is anchored into the outer phospholipid leaflet of the membrane (Fig. 1b and c).

The biological role of β_2GPI is not certain, but it is believed that when inserted in the membrane it is recognized by antiphospholipid antibodies (aPL) [10] which are associated with antiphospholipid syndrome, an autoimmune disease [11]. One possible example of β_2GPI involvement in cellular processes is the formation of apoptotic blebs on cells losing transmembrane lipid asymmetry at the beginning of apoptosis. Abundant quantities of β_2GPI were detected in the blebs [12], suggesting that β_2GPI plays a role *in vivo* in budding and vesiculation of membranes. It could thus act as an immunological marker for macrophages when removing liposomes or apoptotic cells [13]. In an earlier study of interactions of β_2GPI with giant unilamellar vesicles (GUVs) [14], buds were observed to form on the surface of GUVs. Shape transformations of GUVs could thus constitute a promising tool with which to probe the effects of this type of protein on

* Corresponding author. Institute of Biophysics, Faculty of Medicine, University of Ljubljana, Lipičeva 2, 1000 Ljubljana, Slovenia. Tel.: +386 1 543 7603; fax: +386 1 431 5127.
E-mail address: jasna.kovacic@mf.uni-lj.si (J. Kovačič).

0301-4622/$ – see front matter © 2010 Elsevier B.V. All rights reserved.
doi:10.1016/j.bpc.2010.07.005

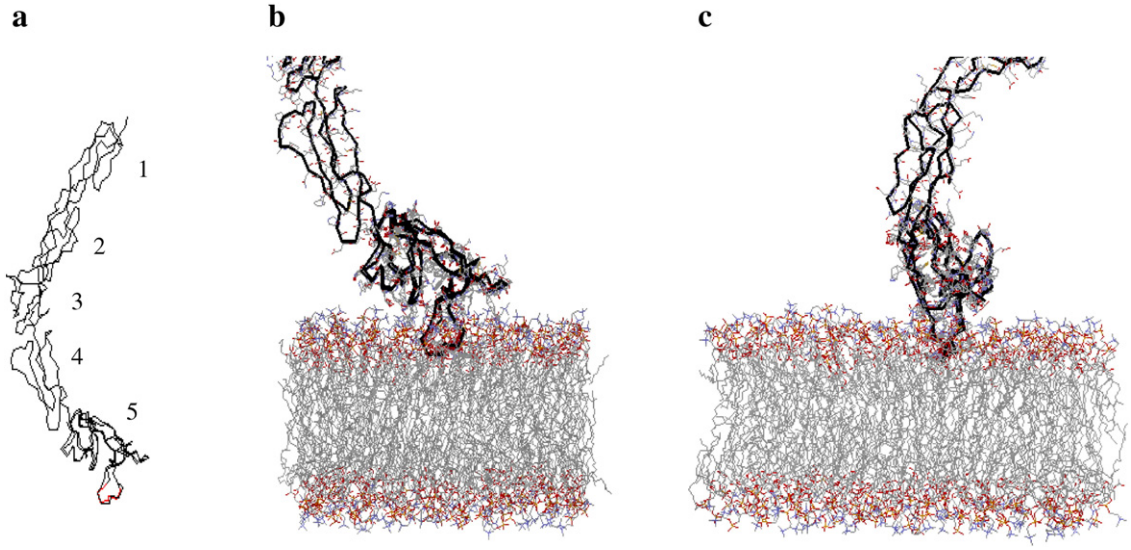

Fig. 1. (a) Schematic representation of β_2GPI (Protein Data Bank Identification Number: 1c1z). The structure shows an extended chain of five domains with an overall fish-hook appearance with the hydrophobic loop on the fifth domain marked in red. (b) The hydrophobic loop embedded in a membrane (the image is obtained with molecular dynamics). (c) View of the hydrophobic loop in the membrane from approximately 90° to that in b which reveals the keel-like part of the inserted portion of the protein at its distal end. It is evident that the majority of the hydrophobic loop of the protein is inserted in the region of polar headgroups of phospholipids and only the keel-like part reaches deeper into where we presume the neutral surface is. The area of the cross-section of the keel-like part is smaller than that of the cross-section of the whole inserted portion of the protein.

membranes, in particular by quantitative evaluation of the shape behaviour of flaccid GUVs in their presence. It is our purpose to identify the vesicle parameters crucial to influencing vesicle behaviour in the presence of β_2GPI. The approach introduced in this study may also be of use in studies of the effects of a variety of other proteins that have been identified to directly bind and deform membranes, e.g. proteins involved in membrane traffic processes [15].

The outline of the paper is as follows: we first present a theoretical background for mechanisms by which the binding of amphitropic proteins to the outer leaflet of membranes affects vesicle shapes. This provides a lead for designing the most informative experiments. The description and outcome of the necessary control experiments are presented in the Supplementary information. The results of the dependence of budding of GUVs on β_2GPI concentration are examined critically in the Discussion section by comparing them with the predictions of the proposed model.

2. Theoretical background

Vesicle budding is a specific example of vesicle shape transformations. The fact that amphitropic proteins affect vesicle shape indicates a coupling between their binding properties and the elastic energy of the membrane. This coupling is manifested by the mutual interdependence of the number of bound proteins and the vesicle shape. Here we shall treat this problem by minimizing free energy of the system (G), which is the sum of the elastic energy of the phospholipid membrane (W) and the free energy of the membrane bound proteins (G_p)

$$G = W + G_p. \tag{1}$$

In defining W we shall take into account that we are concerned with the shape behaviour of flaccid vesicles, i.e. vesicles with excess membrane area with respect to the vesicle volume. Because the membrane is composed of two phospholipid leaflets, the relevant terms of the elastic energy of the vesicle membrane are the membrane-local [16] and non-local [17–20] bending energies, expressed as

$$W = \frac{1}{2}k_c\oint(C_1 + C_2 - C_0)^2 dA_0 + \frac{1}{2}\frac{k_r}{h^2 A_0}(\Delta A - \Delta A_0)^2, \tag{2}$$

where k_c and k_r are the local and nonlocal bending moduli of the bilayer, respectively, C_1 and C_2 are the principal curvatures of the membrane and C_0 is its spontaneous curvature. Integration is over the preferred membrane area A_0. ΔA is the difference between the areas of the outer and the inner leaflets and is given by $\Delta A = h\oint(C_1 + C_2)dA_0$, where h is the distance between the neutral surfaces of the membrane leaflets, and ΔA_0 the preferred (equilibrium) difference between the areas of the outer and the inner leaflets.

The preferred membrane area, A_0, and the preferred area difference, ΔA_0, can be expressed in terms of the number of molecules of membrane components and their areas. Since biological membranes and thus experimental membrane systems are multicomponent, there is a possibility of multiple species of phospholipids in the membrane. We shall treat the case in which the proteins are inserted into the outer leaflet of the symmetrical and laterally homogeneous bilayer membrane. The element of the protein inserted into the outer leaflet increases the preferred area of that leaflet while the preferred area of the inner leaflet remains the same. A_0 and ΔA_0 depend therefore on the number of bound proteins (N_P). The preferred areas of the outer and inner leaflets are then $A_{0,2} = \sum_{i=1}^{n_2} A_{L,i}N_{2,i} + A_pN_p$ and $A_{0,1} = \sum_{i=1}^{n_1} A_{L,i}N_{1,i}$, respectively, with $A_{L,i}$ the area of the ith component of n_2 species of phospholipid molecules in the outer leaflet and of n_1 species of phospholipid molecules in the inner leaflet, $N_{2,i}$ and $N_{1,i}$ the numbers of the ith component of n_2 and of n_1 species of phospholipid molecules in the outer and the inner leaflets, respectively, and A_P the effective area of the protein insertion. The vesicle preferred area is then [19]

$$A_0 = \frac{1}{2}\left(A_{0,2} + A_{0,1}\right) \tag{3}$$

and the preferred area difference is

$$\Delta A_0 = A_{0,2} - A_{0,1}. \tag{4}$$

The protein insertion also affects the spontaneous curvature of the outer leaflet and, consequently, of the membrane (C_0). By taking into consideration the approximation that C_0 depends on the intrinsic curvatures of the protein (C_P) and phospholipid molecules ($C_{L,i}$) of the

ith component of n_2 species of phospholipid molecules in the outer leaflet and of n_1 species of phospholipid molecules in the inner leaflet, the spontaneous curvatures of the outer and inner leaflets are

$$C_{0,2} = \left(\sum_{i=1}^{n_2} N_{2,i}A_{L,i}C_{L,i} + N_pA_pC_p\right)/A_{0,2} \tag{5}$$

and

$$C_{0,1} = \left(\sum_{i=1}^{n_1} N_{1,i}A_{L,i}C_{L,i}\right)/A_{0,1}. \tag{6}$$

The spontaneous curvatures of the two leaflets thus differ, with a consequent non-zero bilayer spontaneous curvature [19]

$$C_0 = \frac{1}{2}\left(C_{0,1} + C_{0,2}\right), \tag{7}$$

and C_0 is proportional to the difference $C_P - C_L$. The elastic energy of the system (W) is equal at given N_p and A_p, if $A_{0,1}$, $A_{0,2}$ and C_0 of different membranes are equal, regardless of the number of membrane components. For the sake of simplicity we therefore define the mean area of phospholipid molecules $A_L = \sum_{i=1}^{n_2} A_{L,i}N_{2,i}/N_2$, where N_2 is a total number of phospholipid molecules in the outer leaflet of the membrane.

The free energy of proteins bound to the membrane (G_p), can be written in the form [21]

$$G_p = -\varepsilon N_p - kT\left(N_0\ln N_0 - N_p\ln N_p - \left(N_0 - N_p\right)\ln\left(N_0 - N_p\right)\right), \tag{8}$$

where ε represents the energy of the interaction between the protein and the membrane, N_0 is the maximal number of its binding sites, k is Boltzmann constant and T the absolute temperature.

The equilibrium configuration of the vesicle can be obtained by minimizing Eq. (1). Minimization with respect to the number of bound proteins (N_p) is considered first where bound proteins are in equilibrium with the external protein solution. This equilibrium is obtained by equating the chemical potential of bound proteins with that of free proteins

$$\partial G/\partial N_p = \mu_0 + kT\ln(c/c_0), \tag{9}$$

where μ_0 and c_0 are constants and c is the protein concentration of the outer solution. From Eq. (9) N_p is obtained as a function of c

$$N_p = \frac{N_0 c}{K_D + c} \tag{10}$$

where

$$K_D = K_{D,0}e^{\left(dW/dN_p\right)/kT} \tag{11}$$

with

$$K_{D,0} = c_0 e^{-\frac{\mu_0 + \varepsilon}{kT}}. \tag{12}$$

$K_{D,0}$ is a shape independent part of the binding constant.

Minimization with respect to vesicle shape can be carried out at fixed values of vesicle volume and of numbers of lipid molecules and of proteins inserted in the membrane. Since G_P does not explicitly depend on vesicle shape, only W has to be minimized. The result of the minimization of W is the vesicle shape and the relation between ΔA and ΔA_0 [20,22,23]. The number of inserted molecules depends on vesicle shape, because the elastic energy depends on N_p. Therefore K_D (Eq. (11)) depends on ΔA, i.e. on vesicle shape. The vesicle shapes at relatively large ΔA_0 values are approximated well by a spherical main vesicle body and spherical buds that may also be arranged as strings [24]. The fact that vesicle shapes, that are compositions of spheres, may have only two different radii is taken into account [25].

We first determine how budding progresses as a function of the external concentration of the amphitropic protein, by approximating the vesicle shapes as being composed of the main spherical body and n spherical buds. At fixed vesicle volume and solution concentration, its shape and N_p depend only on n because the radii of spheres and the corresponding difference between the areas of the outer and the inner leaflets (ΔA) depend only on the number of buds. ΔA is expressed by $8\pi hR_v + n8\pi hR_n$, with R_v the radius of the main spherical body and R_n the radius of the bud. By assuming that the number of buds is an increasing function of the concentration, the number of buds increases from n buds to $n+1$ buds at concentrations at which the free energies of the system (Eq. (1)), calculated separately for n and $n+1$ buds, assume equal values. In this procedure N_p is obtained from Eq. (10) separately for shapes with n and $n+1$ buds. The budding is found to depend on the degree of flaccidness, which is conveniently measured by the reduced volume, defined as the ratio of vesicle volume (V) to volume of the sphere with the same membrane area (A_0),

$$v = \frac{3V}{4\pi R_0^3} \tag{13}$$

where R_0 is the radius of a sphere with the same membrane area $\left(R_0 = \sqrt{A_0/4\pi}\right)$.

The dependence of the number of buds (n) on the reduced volume (v), on the radius of a sphere with the same membrane area (R_0) and on the reduced concentration ($c/K_{D,0}$), is shown in Fig. 2. Fig. 2a is a phase diagram showing the dependence of the number of buds (n) on reduced volume (v) and reduced protein concentration ($c/K_{D,0}$). Each zone limited by two neighbouring curves defines a certain number of buds. At each transition n is increased by one. Every time the vesicle undergoes a transition from n to $n+1$ buds, the bud size is reduced because area and volume redistribute. At given $c/K_{D,0}$, for spherical vesicles (v close to 1) significantly less pronounced shape transformations (lower n) are predicted than for flaccid vesicles ($v<1$). Vesicles with higher v have smaller buds than those with lower v but the same number of buds. At a given value of v the final number of buds is limited, because of the limited maximal number of binding sites on the vesicle. Fig. 2b shows the dependence of the number of buds (n) on reduced concentration ($c/K_{D,0}$) for different values of vesicle size (R_0). It is evident that, at a given β_2GPI concentration, larger vesicles can produce more buds than smaller vesicles. At larger R_0 more buds are formed, due to an increase in ΔA_0 which increases proportionally to R_0^2 (Eq. (4)) because N_P is approximately proportional to N_2, while ΔA at the same shape increases proportionally to R_0.

3. Design of the experiment

The purpose here is to study the properties of the binding of β_2GPI to membranes and the influence of such binding on the shape of an individual vesicle, observed under a phase contrast microscope. Shape transformations of the chosen vesicle should not be disturbed by other vesicles, e.g. due to β_2GPI induced aggregation of anionic vesicles [26]. Also the lipid:β_2GPI ratio should be in favour of β_2GPI. A procedure to isolate chosen vesicles from the pool of vesicles by transferring them in the desired solution was therefore employed [14,24,27], modified because in our experiments we were interested in the β_2GPI concentration dependence of shape transformations of vesicles. β_2GPI, in this case, was injected into the solution with the isolated vesicle so that the outer concentration increased only slowly with time.

Shape transformations should be as extensive as possible in order to observe them under the microscope. The phase diagram in Fig. 2a shows the dependence of the number of buds on v and $c/K_{D,0}$, and it can be seen that the shape transformations are more pronounced for

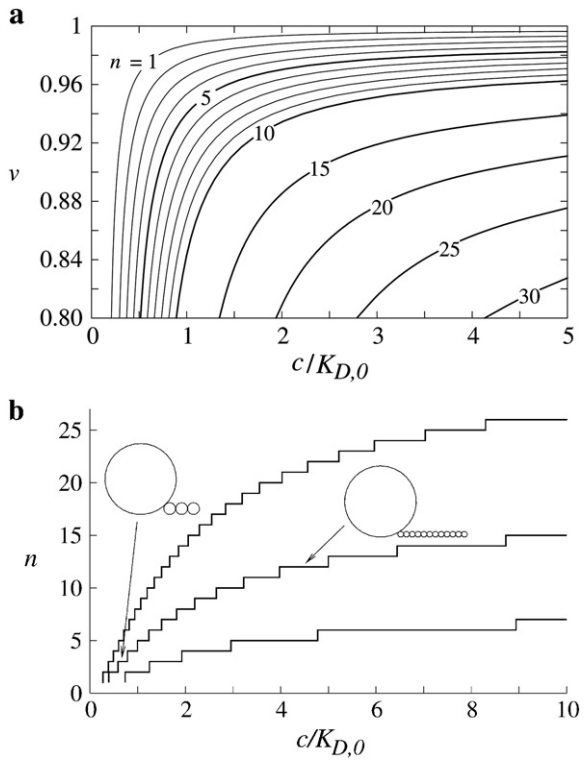

Fig. 2. Theoretically predicted dependence of the number of buds (n) on the reduced volume (v), the radius of a sphere with the same membrane area (R_0), and the reduced concentration ($c/K_{D,0}$) obtained by solving Eqs. (2) and (10). The model parameters are chosen as $A_p = 0.1$ nm^2, $A_L = 0.6$ nm^2, $N_0/N_2 = 0.012$, and $k_r/k_c = 3$. The equilibrium area difference between outer and inner leaflets without intercalated proteins is taken to be equal to the area difference of the sphere ($8\pi h R_0$). (a) The curves of the phase diagram show the transition between n and $n+1$ buds for $R_0 = 20$ μm. (b) The number of buds (n) as a function of $c/K_{D,0}$ for vesicles of different sizes. The radii of spheres with the same membrane area (R_0) are 20 μm (upper curve), 15 μm (middle curve) and 10 μm (lower curve). The reduced volume (v) is 0.9. The cartoons show the shapes of vesicles with various numbers of buds. Note the size of buds is smaller at higher numbers of buds.

flaccid vesicles, which were therefore used in our experiments. The use of flaccid vesicles is also advantageous because the curves are steeper in the region of lower v and thus the accuracy of its value is not so critical for the dependence of budding on $c/K_{D,0}$.

Determination of vesicle dimensions is one of key elements of the study. Vesicles floating in the solution are hard to follow and observe microscopically, and it follows that their size and flaccidity cannot be easily characterized. In order to determine their shape, vesicles were stabilized by falling to the bottom of the observation chamber. This is achieved by creating a difference in density between the fluids inside and outside the vesicle, using different sugars with equal osmolarities but different specific weights.

4. Materials and methods

4.1. Materials and equipment

Purified β_2GPI was isolated and donated by the Department of Rheumatology, University Medical Centre, Ljubljana, Slovenia. D(+)-glucose and D(+)-sucrose were from Fluka, Switzerland. Phospholipids POPC (1-palmitoyl-2-oleoyl-sn-glycero-3-phosphocholine) and POPS (1-palmitoyl-2-oleoyl-sn-glycero-3-phosphoserine) were obtained from Avanti Polar Lipids, USA. Bovine serum albumin (BSA) was from Sigma, USA. Rat blood for the isolation of haemoglobin was donated by the Institute of Pathophysiology, Faculty of Medicine, University of Ljubljana, Slovenia. The ingredients of acid–citrate – dextrose (1:1) anticoagulant, citric acid and dextrose were from Fluka, Switzerland, and sodium citrate was from Riedel-de Haën, Germany. All the solutions were prepared in double-distilled and sterile water. An Olympus IMT2 (USA) inverted microscope, (40x objective, NA = 0.55), was used for phase contrast microscopy. It was equipped with a black and white CCD camera Hammamatsu, C4742-95 (Japan) for image acquisition. Images of vesicles were analyzed with Hammamatsu Hokawo 210 and Image J version 13.6b softwares. The dimensions of the intercalated part of β_2GPI as shown in Fig. 1 were analyzed by RasWin software. Protein solutions were injected into the pit of the observation chamber by a Genie Plus syringe pump (Kent Scientific, USA).

4.2. Preparation of β_2GPI

β_2GPI was purified from pooled human plasma and checked by polyacrylamide gel electrophoresis [28]. Prior to use it was dialyzed against 0.22 M glucose solution, first in a 2 L flask with vortexing for 2 h and then in a fresh glucose solution overnight at +4 °C. The pH value was 8.7 where affinity of β_2GPI towards membrane is sufficiently high [8]. The pH remained stable for several hours.

4.3. Preparation of flaccid vesicles

We used giant unilamellar vesicles (GUVs) composed of 80 mol% neutral POPC and 20 mol% negatively charged POPS. The lipid composition was chosen in order to allow β_2GPI to bind to the vesicles in an electrostatic manner. Preparation of flaccid vesicles took place in two stages: (i) GUVs were prepared using electroformation according to a modification of the method [29]. The protocol for preparation of GUVs was described in ref. [14]. GUVs prepared in such a manner are preferentially spherical, 30 to 60 μm in diameter, filled with 0.2 M sucrose solution and surrounded by isoosmolar glucose/sucrose (1:1) solution. The GUVs were stored at a room temperature for a day to allow time to get rid of abnormalities (tethers, tubes, etc.) that might have resulted during the procedure in electroformation. (ii) Selected GUVs were then transferred using a micropipette into a hyperosmolar (0.22 M) glucose solution to give suitable flaccid vesicles which were recognized by the distinct membrane fluctuations. See Supplementary information for details on preparation of flaccid vesicles, determination of shapes of flaccid vesicles and the influence of gravity and micropipette transfer technique.

4.4. Injection experiments

A pipette (diameter 480 μm), tightly connected by a thin rubber tube to a syringe pump, was inserted into the pit of the observation chamber containing the vesicle under examination in 40 μL of 0.22 M glucose solution. The micropipette was filled with 50 μM β_2GPI in 0.22 M glucose solution. The tip of the pipette was placed in the upper corner of the pit at the maximal distance from the vesicle, which was as a rule released from the pipette close to the other end at the entrance to the pit. β_2GPI was then injected at three intervals as follows. 5 μL of β_2GPI were injected into the solution containing the examined vesicle over 150 s followed by a pause of 150 s to allow the concentrations to equalize. The images of the vesicle during the injection interval were recorded by a camera mounted on a microscope. After the end of each injection the pipette was kept in the pit to avoid disturbing the vesicle. The whole experimental procedure lasted about an hour and during this time no influence of evaporation on v was detected. All experiments were conducted at room temperature. See Supplementary information for details on control experiments.

5. Results

Shape transformations of individual flaccid vesicles were monitored. 17 vesicles were examined, of which about 50% underwent no visible shape transformations, some of which formed protrusions, e.g.

Table 1
Experimentally based and theoretically determined values of vesicle parameters. Values are means ± standard deviation.

Vesicle	R_v (μm)	Z (μm)	n_f	R_0 (μm)	v
A	21.7 ± 0.35	3.4 ± 1	21	19.65 ± 0.4	0.83 ± 0.015
B	18.2 ± 0.3	3.4 ± 1	19	16.6 ± 0.35	0.84 ± 0.02
C	20.65 ± 0.35	7.65 ± 1	9	19.6 ± 0.35	0.895 ± 0.015
D	16.85 ± 0.35	10.2 ± 1	6	16.5 ± 0.35	0.95 ± 0.015
E	11.4 ± 0.25	5.1 ± 1	6	10.95 ± 0.3	0.915 ± 0.025

R_v represents the radius of the ring around the rim of the vesicle and Z the distance from the rim of the vesicle to the substrate, n_f is the final number of observed buds, R_0 is the radius of a sphere with the same membrane area and v is the reduced volume.

tubes. The largest group of vesicles however formed buds. Five of these were selected for detailed analysis for having buds sufficiently visible to be reliably counted. The radius of the ring around the rim of the vesicle (R_v), the distance from the rim of the vesicle to the substrate (Z) (the method of their determination is presented in the Supplementary information) and the final number of buds (n_f) for these vesicles (A–E) are listed in Table 1. The radius of a sphere with the same membrane area (R_0) and the reduced volume (v), calculated from the foregoing parameters, as described in the Supplementary information, are also listed.

The time course of budding of vesicle B after the start of β_2GPI injection is shown in Fig. 3. Budding started to be visible after a time lag of 207 s. During this time the vesicle did not change shape. Buds were then ejected in a consecutive way from multiple membrane sites like strings of buds, as indicated on the image at 600 s. The first budding series, occurring in the time interval 207 s–221 s, shown by an arrow at twelve o´clock position, consisted of three buds. The second series, of 5 buds (236 s–278 s), occurred at five o´clock position, and the third, out of 11 buds (317 s–606 s), at eight o´clock position. The sizes of the buds in the second and third budding series were smaller than those in the first. Other vesicles exhibited similar behaviour, except that occasionally, e.g. vesicle C, strings of buds grew in parallel. Vesicles with smaller v in general exhibited more buds on strings than those with higher v. The latter usually had only one or a few buds on a string and tended to bud individually from many sites. It was also observed that later in time (not shown) some buds detached from the main vesicle body or from each other.

The time dependence of the number of buds (n) formed by membranes of vesicles A to E is shown in Fig. 4. The dashed curve shows the increase of β_2GPI concentration averaged over the whole chamber volume, i.e. as if it were uniformly distributed at all times. n increased with β_2GPI concentration for all vesicles, in steps according to the injection intervals, eventually reaching a plateau. For some vesicles (like A and B) the steps were very steep. Buds were formed successively following injection steps. However, some vesicles, like vesicle D, did not start budding before the second injection interval. There was a time lag in the onset of budding after the start of injection, and budding was still occurring after the injection stops. The behaviour of vesicles is characterized by R_0 and v. For example, case B had significantly higher final number (n_f) of buds and significantly lower v than case D which had a similar R_0. For vesicles with higher v and the same R_0, n_f was lower at the same protein concentration, indicating that more β_2GPI had to be embedded in the membrane to create the same number of buds. Moreover, larger vesicles (higher R_0) also produced more buds than smaller vesicles with the same v.

R_v was observed to depend on n for all vesicles A to E (Fig. 5). R_v at the beginning and during the process of budding was measured where a decrease in that radius could have been observed after an increase in n.

6. Discussion

The previous qualitative study of the formation of buds on the surface of giant unilamellar vesicles (GUVs) in the presence of β_2GPI

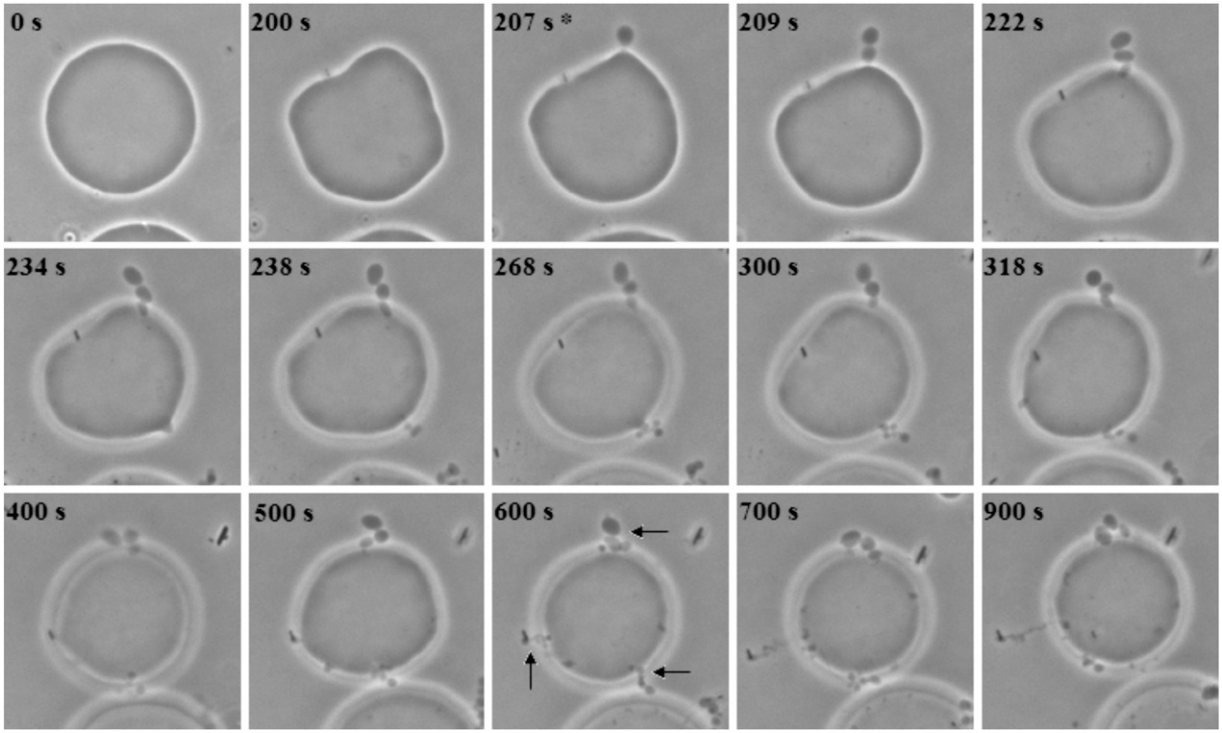

Fig. 3. A typical example of shape deformations of flaccid vesicles during injection of β_2GPI (vesicle B from Table 1 is presented). The time from the beginning of injection is indicated. Arrows (at 600 s) show three budding sites with multiple buds ejected from the membrane. Three buds were produced on the first budding site (207 s–221 s), five on the second budding site (236 s–278 s), and 11 on the third budding site (317 s–606 s). Certain images of the main vesicle body are out of focus in order to show in focus protrusions which are normally present below the rim of the main vesicle body, i.e. on the substrate due to gravity. * designates the onset of budding.

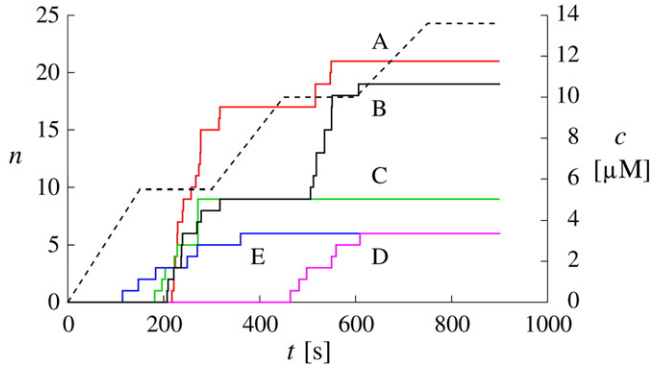

Fig. 4. The time dependence of the observed number of buds (n) on vesicles A to E (Table 1) during the injection of β_2GPI in three intervals (0–900 s overall). The dashed curve represents an average concentration of β_2GPI which rises according to the injections (0 s–150 s, 300 s–450 s and 600 s–750 s).

and their dependence on the vesicles' state led to the suggestion that buds form because insertion of β_2GPI into the outer membrane leaflet increases the area of that leaflet, resulting in curvature enhancement and consequent vesicle shape transformations [14]. In our research we investigated the shape behaviour of individual vesicles when introduced to a solution with β_2GPI at increasing concentrations in a more quantitative way by defining vesicle parameters. First we will discuss the adequacy of the experimental methods. The experimental work will then be analyzed with respect to the theoretical modelling of the shape behaviour of vesicles after the insertion of proteins in the outer membrane leaflet.

GUVs serve as an *in vitro* membrane system as they are cell-sized and can be observed and manipulated under the microscope [30]. However, their use has some drawbacks. They differ from each other (size, flaccidity, lipid composition of both membrane leaflets) because of their inhomogeneity in the original solution as a result of the preparation procedure. Because of their difference, different shape transformations (buds, tubes of different lengths and widths, no shape transformations) are observed during the injection experiment. As shown in Fig. 2a, flaccidity has an important impact on the shape of protrusions. If reduced volume (v) is high enough no shape transformations are formed within the experimental conditions. Also, at higher v smaller buds are observed which eventually could be observed as tubes. It was observed in our experiments that only the most fluctuating vesicles formed buds and the least fluctuating did not change shape. Because of many different possibilities for the shapes of protrusions, the number of investigated vesicles forming countable buds could not be very large. However, because it was our intention to analyze behaviour of individual vesicles in order to recognize crucial vesicle parameters that influence their behaviour and not to study the

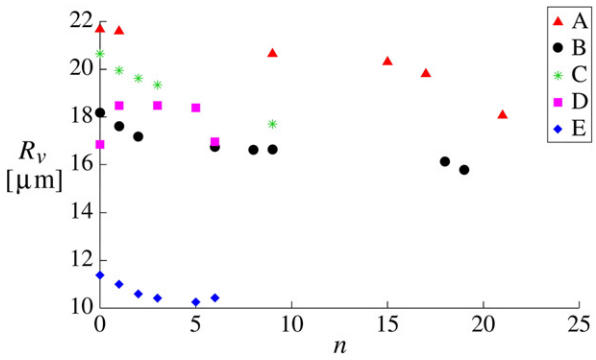

Fig. 5. The dependence of the observed radius of a vesicle at the rim (R_v) on the number of buds (n) for vesicles A–E.

effect on the whole population of vesicles, the need for a high statistical number of cases was not necessary.

While size and v could readily be determined, the initial preferred area difference (ΔA_0) is not easy to establish. Their behaviour is thus to some extent unpredictable. The evidence for unpredictability of vesicles behaviour on account of different initial ΔA_0 seems to be reflected by different time lags of the beginning of budding after the start of injection (Fig. 4); this cannot be explained on the basis of their different radii. Because of different initial values of ΔA_0, a different period of time must pass for β_2GPI to reach a sufficient concentration to reach the ΔA_0 needed to produce a bud leading to the conclusion that the larger the initial ΔA_0 the shorter the time lag. Another drawback of the method is the lack of information about the distribution of β_2GPI molecules throughout the pit of the observation chamber during three consecutive injection intervals because of the unknown rate of liquid mixing. However, based on an injection control experiment of the examination of homogeneity of β_2GPI solution shown in Fig. S3 (Supplementary information), we concluded that the concentration became homogenous before the start of the next injection interval.

A model was proposed having the simplest possible structure that still captures the essential elements of the treated system. The model presumes spherical vesicles with a homogenous surface density of bound proteins. The latter affects not only the preferred area difference (ΔA_0) but also the spontaneous curvature of the membrane (C_0). Both describe the observed shape transformations but in our model we assumed that the effect of ΔA_0 prevails over the effect of C_0. Flip-flop between the leaflets is very slow so we could assume that the preferred areas of membrane leaflets are conserved on the experimentally relevant time scales [31]. According to the bilayer couple hypothesis [25,32], protrusions (buds, tubes, tethers, etc.) of higher membrane curvature on the membrane of the main vesicle body form in order to reduce the difference between ΔA and ΔA_0 and thus the area difference elasticity term of Eq. (2). ΔA depends on the vesicle shape whereas ΔA_0 depends on the molecular occupancy of the two layers and their interaction with the surroundings. These two quantities are generally not identical. The model accounts for the importance of the coupling between vesicle shape and the number of bound proteins (N_p). It assumes that the shape of a vesicle and the number of bound proteins are interdependent. The initial transition of the vesicle shape resulting in the first bud cannot be calculated accurately from the proposed model. All the theoretical results are thus presented from the first bud onwards.

The model predicts the dependence of the number of buds on R_0 and v as shown in Fig. 2a and b. A phase diagram presented in Fig. 6

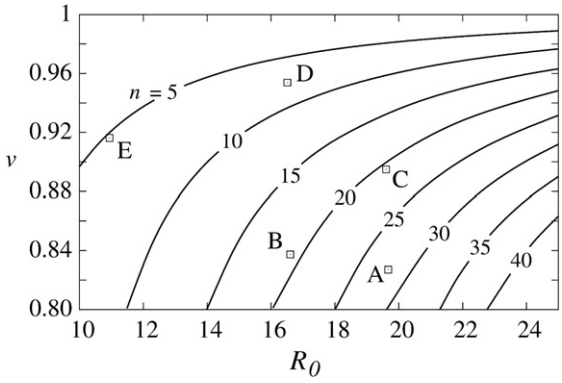

Fig. 6. Phase diagram of the dependence of the number of buds on reduced volume (v) and on the radius of a sphere with the same membrane area (R_0). Experimentally acquired data from vesicles A to E (squares) are positioned on the diagram. The curves show the transition between the theoretically predicted number of buds (n_t, shown by a numerical value on the phase diagram) and n_t+1 for model parameters: $A_p = 0.09$ nm^2, $A_L = 0.6$ nm^2, $N_0/N_2 = 0.012$, $c/K_{D,0} = 10$, and $k_r/k_c = 3$.

combines the effects of parameters R_0 and v on the number of buds. The experimental data (squares) for vesicles A–E were located on this phase diagram. By solving Eqs. (2) and (10) the curves that indicate the theoretically predicted number of buds for certain model parameters were also added to the phase diagram, to test whether the experimental observations of the final number of buds (n_f, Table 1) are in accord with theoretical predictions. If we consider maximal binding of β_2GPI to planar phospholipid membranes ($=0.17\ \mu g/cm^2$) [6] and the mass of one β_2GPI molecule ($=8.3\cdot10^{-11}$ ng), we can calculate the maximal number of proteins (i.e. the maximal number of binding sites) on a vesicle with a typical radius of 20 μm ($N_0=1.02\cdot10^8$). For the model parameters therefore we chose values of the ratio between the maximal number of binding sites and the total number of phospholipid molecules in the outer leaflet ($N_0/N_2=0.012$), the mean area of phospholipid molecules ($A_L=0.6\ nm^2$ [33]), the ratio between nonlocal and local bending moduli of the bilayer ($k_r/k_c=3$), and reduced concentration ($c/K_{D,0}=10$). The reduced concentration was selected according to the conditions close to saturation, i.e. 10 times $K_{D,0}$. At this high protein concentration, the theoretically predicted number of buds was approximated closely to a final number of buds, and the shape of the main vesicle body was approximated to a sphere. We took as an adjustable parameter the effective area of the cross-section of the inserted portion of the protein (A_p) obtained from Eq. (4), which influences ΔA_0, and tried to obtain as good as possible fit with experimental points by varying its value. The position of the curves is greatly dependent on A_p. At values of A_p larger than that estimated, the curves would shift towards the left, because transitions would occur sooner. A_p was, in our case, determined to be about one tenth of the area of the cross-section of the whole inserted portion of the protein. The membrane area thus responsible for ΔA_0 is smaller than that of the whole inserted portion of the protein. The result suggests that only the keel-like part of the inserted portion of the protein (Fig. 1c) reaches the neutral surface of the leaflet and is thus responsible for the increase of ΔA_0. The theoretical predictions of the number of buds agree with experimental results of most vesicles (vesicles A, B, D and E) sufficiently well for the chosen parameters. However the predicted value of n_f for vesicle C deviates slightly from the observed value (discussed later).

The radius of the main vesicle body at the rim (R_v) was determined, as well as the number of buds (n). The dependence on n of the experimental values of R_v for vesicles A–E is presented in Fig. 5, showing that R_v decreases with increasing n. This observation does not fit with the proposed theoretical model, which predicts a slight increase of R_v with bud formation, because the formation of buds involves relatively more increase in vesicle area than in volume. The observations can be understood if it is taken into account that gravity causes a vesicle lying on the substrate to flatten, so that R_v is larger than that of a sphere with the same membrane area (Fig. S1a — Supplementary information). The decrease in R_v with increasing n can be explained by the fact that the volume and membrane area of the newly formed bud are accompanied by their decrease in the main vesicle body. The latter then reforms its shape stepwise from a sphere section into a sphere, which involves an increase in the effective reduced volume of the main vesicle body. When the latter attains the shape of a sphere, the predicted outcome is practically the same as that obtained by the simple theoretical model (Fig. S1b — Supplementary information).

The dependence of R_v on n obtained from measured data for vesicle B (circles) is compared with possible theoretical interpretations (curves) of vesicle behaviour (Fig. 7). The theoretical reasoning described in the section on theoretical background predicts a decrease in R_v represented by the dashed curve. This decrease is quite rapid so that the shape of the sphere is reached at $n=6$, whereas the experimental dependence of R_v on n is much less steep. An attempt is made to interpret the vesicle behaviour by assuming partially closed and closed necks between the main vesicle body and buds. An

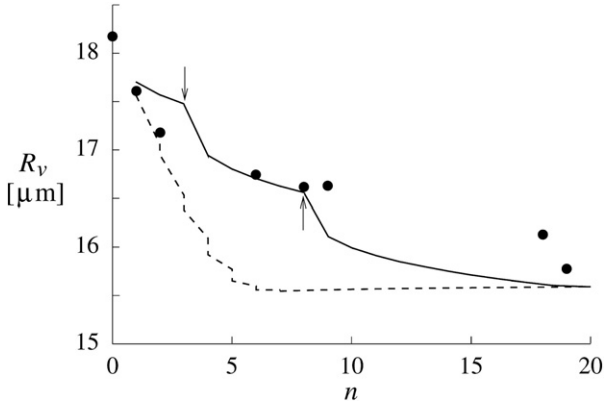

Fig. 7. The dependence of the radius of a vesicle at a rim (R_v) on the number of buds (n). Experimental values for vesicle B are shown by circles and theoretical predictions for model parameters: $A_p=0.09\ nm^2$, $A_L=0.6\ nm^2$, $N0/N_2=0.012$, $k_r/k_c=3$, and $\Delta\rho=15\ kg/m^3$ by curves. The reduced volume of the first protrusion was defined as the ratio between the volume of the first protrusion and the volume of the sphere with the membrane area A_0 is 0.003. The dashed curve describes the interpretation according to the simple theoretical model with gravity. The shape of the sphere is reached at n = 6. The solid curve describes the possible interpretation with partially closed and closed necks (see text). An arrow oriented downwards depicts the transition between the first and second budding sites after three buds, and an arrow oriented upwards depicts the transition between second and third budding site after eight buds. The shape of the sphere is reached at $n=19$.

example is presented by the solid curve. It is assumed that, during the formation of a string of three buds on the first budding site (Fig. 3), the neck is partially closed so that membrane, but not solution inside the vesicle, can be exchanged between the main vesicle body and buds. R_v decreases more slowly than in the case of exchange of both membrane area and solution. It appears that the neck of the first budding site then closes completely (denoted by an arrow at $n=3$), indicating that neither the volume nor the area could be exchanged and that the budding from this budding site stopped. When the second budding site opens, the shift of R_v is again larger (between $n=3$ and 4). During the formation of another string of five buds on the second budding site the neck is, as previously assumed, partially closed and R_v thus decreases correspondingly slowly. An arrow positioned at $n=8$ indicates another possible neck closure. When the third budding site opens, the shift of R_v is again larger (between $n=8$ and 9) and decreases slowly until formation of the last bud ($n=19$) when the shape of the main vesicle body assumes the shape of a sphere. The partial neck closure can be explained by an assumption that solution molecules inside the vesicle cannot move through the neck from the main vesicle body to a protrusion while the membrane components can. The plausible rationale for a total prevention of movement of all molecules through the neck is that the neck gets too narrow. The reason for the neck closure cannot be totally clarified. This interpretation considering closed and partially closed necks was therefore used only to describe observed phenomena properly. A similar interpretation can also be employed to explain the smaller final number of buds (n_f) observed on vesicle C than is predicted theoretically. Budding of this vesicle may have stopped prematurely because the energy barrier for a new bud was too high after the neck closed at some point. However, in this case it may also be that undetected tethers or other protrusions were formed in addition to buds, resulting in a smaller final number of buds.

The interpretation represented by the solid curve in Fig. 7 is consistent with the rapid increase in number of buds seen in Fig. 4 in cases A and B. The predicted dependence of n on $c/K_{D,0}$ for vesicle B is shown in Fig. 8. The lower curve represents the beginning of budding of the initial vesicle that ends at $n=3$. When budding begins on the second budding site, it does not continue on the same curve but rather jumps (shown by a lower arrow) to the middle curve which corresponds to a

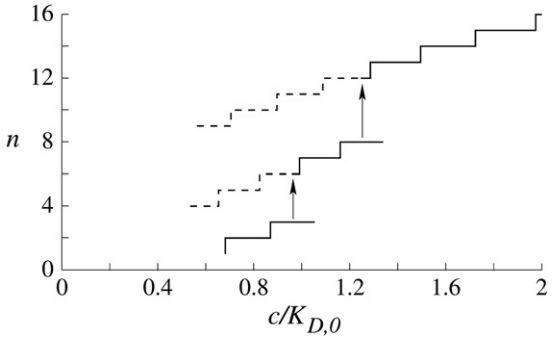

Fig. 8. Theoretical predictions of the dependence of the (total) number of buds (n) on reduced concentration ($c/K_{D,0}$) for the same model parameters as in Fig. 7. The possible steep increase in the number of buds for vesicle B is illustrated. The lower curve represents the start of budding up to $n=3$. After that, budding continues with a jump (shown by a lower arrow) to the middle curve where the number of buds immediately increases for three to four buds. The solid section of the curve depicts the actual course of budding. The dashed section of the curve depicts the imaginary budding path if the jump had not occurred for vesicles with different dimensions. The event repeats with the second jump (shown by an upper arrow) to the upper curve where more buds immediately occur.

now different effective reduced volume of the main vesicle body. This is because the main vesicle body acts as a separate entity and its effective reduced volume is larger, as discussed previously. As the budding continues at the second budding site, the number of buds predicted for the current concentration is already greater than 1 and the number of buds immediately increases to a total of six or seven. The budding continues on the solid section of the middle curve as long as the neck closes again. The analogous interpretation applies when the third budding site opens, with the result that the possible interpretation of budding jumps to the upper curve. The budding continues on the solid section of the upper curve where at $n=19$ a spherical shape is reached. In accord with the interpretation of the steep increase of the number of buds seen in Fig. 4 for vesicles exhibiting long strings of buds (A and B), and in vesicles where budding is individual (D and E), the number of buds increases in steps.

7. Conclusions

The notion that β_2GPI induces shape transformations of vesicles preferentially by forming buds and strings of buds is confirmed in this study. The extent of budding is an increasing function of β_2GPI concentration. The occurrence of budding can be rationalized by assuming that part of β_2GPI is inserted only into the outer leaflet of the bilayer, thus increasing the preferred difference between the areas of the outer and the inner leaflets (ΔA_0). The contribution to ΔA_0 of each bound β_2GPI was estimated to be about one tenth of the area of the cross-section of its inserted portion, meaning that only a part of it reaches into the neutral surface of the leaflet and is involved in changing ΔA_0. By combining theoretical modelling of the shape behaviour of vesicles with experimental results for a number of vesicles it was deduced that, at a given β_2GPI concentration, the greater number of buds is characteristic of more flaccid (lower volume to area ratio) and larger vesicles. When the vesicle membrane is under stress, e.g. lying on the substrate as a result of gravity, a larger β_2GPI concentration is needed to produce the same degree of budding relative to the unstrained vesicle. Particularly under conditions of gravity, different vesicles behave differently because the neck between the main vesicle body and buds or strings of buds can be either closed or open. The qualitative and quantitative insights presented here into the process of budding and vesiculation of vesicles could have an application when studying the binding properties of other amphitropic proteins to biological membranes.

Acknowledgements

We thank Prof. Blaž Rozman, PhD (Department of Rheumatology, University Medical Centre, Ljubljana, Slovenia) for providing the purified β_2GPI, Prof. Robert Zorec, PhD (Institute of Pathophysiology, Faculty of Medicine, University of Ljubljana, Slovenia) for providing the rat blood, Prof. Jure Stojan, PhD (Institute of Biochemistry, Faculty of Medicine, University of Ljubljana) for providing the images of β_2GPI embedded in the membrane. We are also grateful to Janja Majhenc, PhD (Institute of Biophysics, Faculty of Medicine, University of Ljubljana) for the valuable discussions. This work was supported by Slovenian Research Agency through grant no. P1-0055.

Appendix A. Supplementary data

Supplementary data to this article can be found online at doi:10.1016/j.bpc.2010.07.005.

References

[1] P. Burn, Amphitropic proteins: a new class of membrane proteins, Trends Biochem. Sci. 13 (1988) 79–83.
[2] J.E. Johnson, R.B. Cornell, Amphitropic proteins: regulation by reversible membrane interactions (review), Mol. Membr. Biol. 16 (1999) 217–235.
[3] B. Bouma, P.G. de Groot, J.M.H. van den Elsen, R.B.G. Ravelli, A. Schouten, M.J.A. Simmelink, R.H.W.M. Derksen, J. Kroon, P. Gros, Adhesion mechanism of human β2-glycoprotein I to phospholipids based on its crystal structure, EBMO J. 18 (1999) 5166–5174.
[4] A. Steinkasserer, P.N. Barlow, A.C. Willis, Z. Kertesz, I.D. Campbell, R.B. Sim, D.G. Norman, Activity, disulfide mapping and structural modeling of the fifth domain of human β2-glycoprotein I, FEBS Lett. 313 (1992) 193–197.
[5] H. Wurm, β2-glycoprotein-I (apolipoprotein H) interactions with phospholipids vesicles, Int. J. Biochem. 16 (1984) 511–515.
[6] G.M. Willems, M.P. Janssen, M.M.A.L. Pelsers, P. Comfurious, M. Galli, R.F.A. Zwaal, E.M. Bevers, Role of divalency in the high-affinity binding of anticardiolipin antibody β2-glycoprotein I coplexes to lipid membranes, Biochemistry 35 (1996) 13833–13842.
[7] M.F. Harper, P.M. Hayes, B.R. Lentz, R.A.S. Roubey, Characterization of β2-glycoprotein I binding to phospholipid membranes, Thromb. Haemost. 80 (1998) 610–614.
[8] S.X. Wang, G. Cai, S. Sui, The insertion of human apolipoprotein H into phospholipid membranes: a monolayer study, Biochem. J. 335 (1998) 225–232.
[9] R. Gamsjaeger, A. Johs, A. Gries, H.J. Gruber, C. Romanin, R. Prassl, P. Hinterdorfer, Membrane binding of β2-glycoprotein I can be described by a two-state reaction model: an atomic force microscopy and surface plasmon resonance, Biochem. J. 389 (2005) 665–673.
[10] M. Galli, P. Comfurius, C. Maasen, H.C. Hemker, M.H. Debiets, P.J.C. Van Bred-Vriesman, T. Barbui, R.F.A. Zwaal, E.M. Bevers, Anticardiolipin antibodies directed not to cardiolipin but to a plasma protein cofactor, Lancet 335 (1990) 1544–1547.
[11] H.P. McNeil, R.J. Simpson, C.N. Chesterman, S. Krillis, Antiphospholipid antibodies are directed against a complex antigen that includes a lipid-binding inhibitor of coagulation: β2 glycoprotein I (apolipoprotein H), Proc. Natl Acad. Sci. USA 87 (1990) 4120–4124.
[12] L. Casciola-Rosen, A. Rosen, M. Petri, M. Schlissel, Surface blebs on apoptotic cells are sites of enhanced procoagulant activity: implications for coagulation events and antigenic spread in systemic lupus erythematosus, Proc. Natl Acad. Sci. USA 93 (1996) 1624–1629.
[13] J. Connor, C.C. Pak, A.J. Schroit, Exposure of phosphatidyserine in the outer leaflet of human red-blood-cells — relationship to cell-density, cell age, and clearance by mononuclear-cells, J. Biol. Chem. 269 (1994) 2399–2404.
[14] A. Ambrožič, B. Božič, T. Kveder, J. Majhenc, V. Arrigler, S. Svetina, B. Rozman, Budding, vesiculation and permeabilization of phospholipids membranes — evidence for a feasible physiologic role of β2-glycoprotein I and pathogenic actions of anti-β2-glycoprotein I antibodies, Biochim. Biophys. Acta 1740 (2005) 38–44.
[15] K. Farsad, P. De Camilli, Mechanisms of membrane deformation, Curr. Opin. Cell Biol. 15 (2003) 372–381.
[16] W. Helfrich, Elastic properties of lipid bilayers — theory and possible experiments, Z. Natturforsch. C 28 (1973) 693–703.
[17] W. Helfrich, Blocked lipid exchange in bilayers and its possible influence on shape of vesicles, Z. Natturforsch. C 29 (1974) 510–515.
[18] E.A. Evans, Minimum energy analysis of membrane deformation applied to pipet aspiration and surface-adhesion of red-blood-cells, Biophys. J. 30 (1980) 265–284.
[19] S. Svetina, M. Brumen, B. Žekš, Lipid bilayer elasticity and the bilayer couple interpretation of red-cell shape transformations and lysis, Stud. Biophys. 110 (1985) 177–184.
[20] L. Miao, U. Seifert, M. Wortis, H.G. Döbereiner, Budding transitions of fluid-bilayer vesicles — the effect of area-difference elasticity, Phys. Rev. E. 49 (1994) 5389–5407.
[21] T.L. Hill, An introduction to Statistical Thermodynamics, Dover Publications, New York, 1986.

[22] V. Heinrich, S. Svetina, B. Žekš, Nonaxisymmetric vesicle shapes in a generalized bilayer-couple model and the transition between oblate and prolate axisymmetrical shapes, Phys. Rev. E 48 (1993) 3112–3123.
[23] M. Jarić, U. Seifert, W. Wintz, M. Wortis, Vesicular instabilities — the prolate-to-oblatetransition and other shape instabilities of fluid bilayer-membranes, Phys. Rev. E 52 (1995) 6623–6634.
[24] B. Božič, G. Gomišček, V. Kralj-Iglič, S. Svetina, B. Žekš, Shapes of phospholipid vesicles with beadlike protrusions, Eur. Biophys. J. 31 (2002) 487–496.
[25] S. Svetina, B. Žekš, Membrane bending energy and shape determination of phospholipid vesicles and red blood cells, Eur. Biophys. J. 17 (1989) 101–111.
[26] F.C. Gushiken, A. Le, F.C. Arnett, P. Thiagarajan, Polymorphisms β2-glycoprotein I: phospholipids binding and multimeric structure, Throm. Res. 108 (2003) 175–180.
[27] M. Mally, J. Majhenc, S. Svetina, B. Žekš, Mechanisms of equinatoxin II-induced transport through the membrane of a giant phospholipid vesicle, Biophys. J. 83 (2002) 944–953.
[28] S. Čučnik, I. Križaj, B. Rozman, T. Kveder, B. Božič, Concomitant isolation of protein C inhibitor and unnicked ß2-glycoprotein I, Clin. Chem. Lab. Med. 42 (2004) 171–174.
[29] M.I. Angelova, S. Soleau, P. Méléard, J.F. Faucon, P. Bothorel, Preparation of giant vesicles by external ac electric fields: kinetics and applications, Prog. Colloid Polym. Sci. 2 (1992) 127–131.
[30] P.L. Luisi, P. Walde, Giant Vesicles: Perspectives in Supramolecular Chemistry, John Wiley & Sons, England, 2000.
[31] H.G. Döbereiner, E. Evans, M. Kraus, U. Seifert, M. Wortis, Mapping vesicle shapes into the phase diagram: a comparison of experiment and theory, Phys. Rev. E 55 (1997) 4458–4474.
[32] M.P. Sheetz, S.J. Singer, Biological membranes as bilayer couples. A molecular mechanism of drug-erythrocyte interactions, Proc. Nat. Acad. Sci. U.S.A. 71 (1974) 4457–4461.
[33] G. Cevc, D. Marsh, Phospholipid Bilayers, John Wiley & Sons, Canada, 1987.